Front. Earth Sci. 2015, 9(1): 1–12
DOI 10.1007/s11707-014-0444-9

RESEARCH ARTICLE

Analysis of spatio-temporal variability of aerosol optical depth with empirical orthogonal functions in the Changjiang River Delta, China

Tianyong ZHAI[1,2], Qing ZHAO (✉)[1,2], Wei GAO[1,2,3], Runhe SHI[1,2], Weining XIANG[4], Hung-lung Allen HUANG[5], Chao ZHANG[1,2]

1 Key Laboratory of Geographic Information Science (Ministry of Education), East China Normal University, Shanghai 200062, China
2 Joint Laboratory for Environmental Remote Sensing and Data Assimilation, ECNU&CEODE, Shanghai 200062, China
3 Colorado State University, Natural Resource Ecology Laboratory, Fort Collins, Colorado 80521, USA
4 Shanghai Key Laboratory for Urban Ecology and Sustainability, East China Normal University, Shanghai 200062, China
5 University of Wisconsin–Madison, Cooperative Institute for Meteorological Satellite Studies (CIMSS), Madison, Wisconsin 53706, USA

© Higher Education Press and Springer-Verlag Berlin Heidelberg 2014

Abstract This work aims to analyze the spatial and temporal variability of aerosol optical depth (AOD) from 2000 to 2012 in the Changjiang River Delta (CRD), China. US Terra satellite moderate resolution imaging spectroradiometer (MODIS) AOD and Ångström exponent (α) data constitute a baseline, with the empirical orthogonal functions (EOFs) method used as a major data analysis method. The results show that the maximum value of AOD observed in June is 1.00±0.12, and the lowest value detected in December is 0.40±0.05. AOD in spring and summer is higher than in autumn and winter. On the other hand, the α-value is lowest in spring (0.86±0.10), which are affected by coarse particles. High α-value appears in summer (1.32±0.05), which indicate that aerosols are dominated by fine particles. The spatial distribution of AOD has a close relationship with terrain and population density. Generally, high AODs are distributed in the low-lying plains, and low AODs in the mountainous areas. The spatial and temporal patterns of seasonal AODs show that the first three EOF modes cumulatively account for 77% of the total variance. The first mode that explains 67% of the total variance shows the primary spatial distribution of aerosols, i.e., high AODs are distributed in the northern areas and low AODs in the southern areas. The second mode (7%) shows that the monsoon climate probably plays an important role in modifying the distribution of aerosols, especially in summer and winter. In the third mode (3%), this distribution of aerosols usually occurs in spring and winter when the prevailing northwestern or western winds could bring aerosol particles from the inland areas into the central regions of the CRD.

Keywords AOD, MODIS, EOFs, Ångström exponent, Changjiang River Delta

1 Introduction

Atmospheric aerosol refers to the liquid or solid particles suspended in the air. These particles play an important role in the earth's energy balance through direct and indirect radiative forcing (Kaufman et al., 2002). They can scatter and absorb solar radiation, and reduce the energy of solar radiation reaching the Earth's surface. They also affect both the processes of cloud formation by acting as cloud condensation nuclei, and the hydrological cycle through changes in cloud cover and properties and levels of precipitation (King et al., 1992, 1999; Kaufman et al., 2002). These changes in the properties and distributions of clouds have an enormous impact on the climate.

In recent years, economic growth and population expansion have increased the amount of aerosol particles in the air through car emissions, industrial processes, and coal-fired heating. Previous studies have shown that fine particles could be the dominant factor affecting human health due to the presence of sulfates, nitrates, and acids (Yang, 2002; Kennedy, 2007). Particulate matter of $\leqslant$2.5 μm in diameter (PM2.5) are breathed more deeply into the lungs, whereas particulate matter of $\leqslant$10 μm in diameter (PM10) can penetrate the thoracic region of the lungs (Pope and Dockery, 2006).These particles can also have a negative impact on the atmosphere by causing a reduction

Received April 11, 2013; accepted January 21, 2014

E-mail: jenniferzhao0510@gmail.com

of atmospheric visibility and a decline in air quality (Qiu and Yang, 2000; Engel-Cox et al., 2004; Li et al., 2005). Even so, the sources of aerosol are diverse. For example, some aerosols are produced by nature, such as wind-blown desert dust or sea salt caused by breaking waves while others are mainly caused by human activities, such as urban industrial pollution and biomass burning (Remer et al., 2005).

Aerosol optical properties, such as aerosol optical depth (AOD), aerosol particle size, single scattering albedo, and refractive index can be used to quantitatively identify the aerosol distributions both in time and space (Kaufman et al., 2002). AOD describes the attenuation of sunlight by a column of aerosol, and thus serves as a measure of aerosol column concentration (Kaufman et al., 2002). Aerosol optical properties can be obtained mainly through ground-based observations or remote sensing monitoring. The simplest, and in principle, the most accurate way to maintain monitoring systems is ground-based (Holben et al., 2001). However, ground-based observations are not suitable at large scales. The regional and global monitoring of aerosols by remote sensing techniques has become widely used as it complements the limitations of ground-based observations. Long-term observation of aerosols through remote sensing could provide a valid method for the understanding of the characterization of aerosols at different spatial and temporal scales (Remer et al., 2005). In addition, satellite remote sensing is suggested to be well-suited for the daily monitoring of the aerosol load because of its large spatio-temporal coverage (Kaufman et al., 2002). The moderate resolution imaging spectro-radiometer (MODIS) is a sensor onboard NASA's Terra and Aqua satellites, which were launched in December 1999 and May 2002, respectively. MODIS can detect aerosol changes and long-term influences on global climate.

It is necessary to distinguish between aerosols from natural resources and anthropogenic sources (Kaufman et al., 2002). To some degree, it is possible that aerosol particle size could be distinguished based on the Ångström exponent (α). The Ångström exponent is commonly used to describe the spectral dependence of AOD and provide some basic information about the aerosol size distribution (Eck et al., 1999; Chu et al., 2002; Kaskaoutis et al., 2006). The Ångström exponent values distinguish between distributions of coarse particles that occur naturally and fine particles that occur anthropogenically (Kim et al., 2013). Its empirical expression (Ångström, 1929) is defined as $\tau(\lambda)=\beta\lambda^{-\alpha}$, where $\tau(\lambda)$ is the AOD for wavelength λ, α is the Ångström exponent, and β is the AOD at a reference wavelength of 1 μm. In order to calculate α, it is common to choose two wavelengths to take the slope of the linear fit to the logarithm of λ and the logarithm of τ. The Ångström exponent is defined as $\ln(AOD_{0.47}/AOD_{0.66})/\ln(0.66/0.47)$ for MODIS over land and $\ln(AOD_{0.55}/AOD_{0.865})/\ln(0.865/0.55)$ over ocean. Generally, the larger the effective radius of an aerosol particle, the smaller α will be (King et al., 1999; Li et al., 2003).

Changjiang River Delta (CRD) is a highly developed urban agglomeration in China. During the past 30 years, the rapid economic development and urban expansion, with increased population density, have had a significant impact on the CRD environment (Duan et al., 2009). Therefore, more attention should be paid to the impact of aerosols in this region (He et al., 2010; Pan et al., 2010). The main objective of this work is to analyze the spatial and temporal distribution of AOD and Ångström exponent from Terra MODIS level 2 aerosol products in the CRD from 2000 to 2013. To further understand the seasonal variability of AOD, the empirical orthogonal functions (EOFs) method is used to process spatial and temporal decomposition, and to attempt to find the main factors influencing the spatial distribution of AOD.

2 Materials and methods

2.1 Study area

CRD (29°N–34°N, 118°E–122°E) is experiencing one of the fastest-growing economies in China (Fig. 1). The area has intensive growth in its population and industry. It is an important part of the middle and lower reaches of the Changjiang River Plain, located to the west of the Yellow and East China Seas. The altitude in this area is shown in Fig. 1. Low-lying plains are mainly distributed in the northern regions of CRD, with the mountainous areas mainly in the south. High mountains can block transportation of aerosol particles by wind. The study area is located in the subtropical monsoon climate zone, characterized by high temperature and rainy climate in the summer, and mild and dry climate in the winter. Thus, the variability of aerosols in the CRD may be affected by many factors.

2.2 Data

MODIS has 36 channels, which cover the visible and thermal-infrared spectrum at three spatial resolutions (250 m, 500 m, and 1 km), with a wide swath (2,330 km). The data presented in this work are collected from MODIS onboard Terra satellite during March 2000 to February 2013. The aerosol products (Level 2 MOD04 Collection 051 daily 0.55 μm aerosol optical depth) observed with the spatial resolution of 10 km can be downloaded from the NASA website (http://ladsweb.nascom.nasa.gov/data/search.html). The MODIS aerosol algorithm retrieves AOD at 0.47 μm, and 0.66 μm wavelengths are based on dark targets over vegetated land surfaces (Kaufman et al., 1997; Remer et al., 2005). Detailed information about algorithm of Collection 005 and 051 is provided by Levy et al. (2009). Further

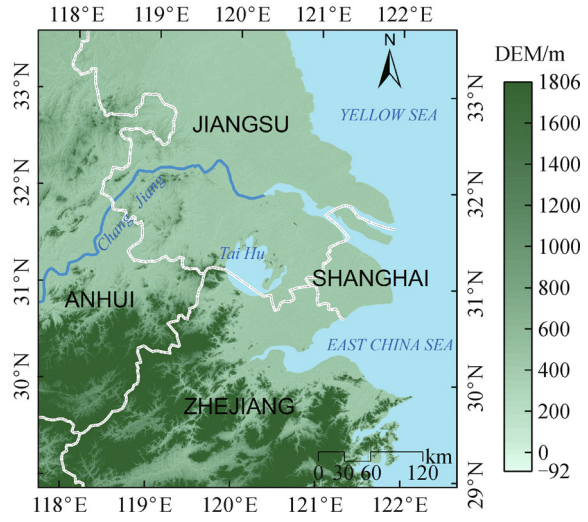

Fig. 1 Location of Changjiang River Delta and its spatial distribution of altitude in meters.

validation of MODIS aerosol products was achieved with the ground-based sunphotometer data. In this respect, AERONET data are very widely used for MODIS aerosol product validation (Holben et al., 1998; Ichoku et al., 2002; King et al., 2003). Remer et al. (2005) found that MODIS retrieves AOD with an accuracy of $\nabla\tau = \pm 0.05 \pm 0.15\tau$ over land. These results suggest that MODIS aerosol products could be used quantitatively for the evaluation of air pollution, fire, and other climatic research. This is also the case for the work done in CRD. He et al. (2010) reported that MODIS AOD data could satisfy our study in the CRD. In this work, two parameters were chosen from MOD04: aerosol optical depth at 550 nm and Ångström exponent at 470/660 nm.

2.3 Methods

Most aerosols are generally regional in nature due to their short lifetime, the regional distribution of the sources, and the variability in their properties. Seasonal meteorological conditions determine how far aerosols could be transported from their sources, in addition to how they distribute vertically in the atmosphere (Kaufman et al., 2002). The AOD inversion derived through remote sensing generally has a close relationship with surface albedo. However, the presence of clouds will affect the AOD inversion. To guarantee the integrity of the data, they will be calculated at different time steps (monthly, seasonally, and annually). Seasons are divided according to the season: spring is March to May (MAM), summer is June to August (JJA), autumn is September to November (SON), and winter is December to February (DJF).

The empirical orthogonal functions (EOFs) method is used to analyze the seasonal dynamics of AOD time series data during the periods of 2000 to 2012. These data are initially processed into the anomaly matrix before obtaining modes and corresponding time weighting coefficients. More detailed information can be found in the section on EOF analysis. EOFs are primarily used to decompose the original variable field into a linear combination of orthogonal functions, and then to form a few unrelated typical modes instead of the original variable field. Each typical mode contains as much information as the original field (Preisendorfer and Mobley, 1988). This method has always been the standard statistical technique used in the geophysical science fields of meteorology and oceanography (Preisendorfer and Mobley, 1988). The main concept of EOFs is that the variable X_{mn} consists of m stations and n observations is expressed as a linear combination of the space eigenvectors and corresponding time coefficients. It can be defined as follows:

$$\boldsymbol{X}_{mn} = \boldsymbol{V}_{mm}\boldsymbol{Z}_{mn}, \tag{1}$$

where the matrix $\boldsymbol{V}_{mm}$ represents the space eigenvectors and $\boldsymbol{Z}_{mn}$ represents the time coefficients. Generally, the first several modes account for a large part of the total variance and can be related to physical phenomena. The structure of modes can be used to explore spatial and temporal coherence. Hu et al. (2008) applied this method to analyze the spatio-temporal variability of TOMS/NASA monthly AOD between 1980 and 2001 in China. Shrestha and Barros (2010) studied the spatial variability of aerosol, clouds, and rainfall in the Himalayas from satellite data based EOFs that analyzed the spatial mode of aerosol variability of aerosols. In this work, the EOF method is used for the analysis of the spatial and temporal variability of seasonal AOD in-depth in the CRD.

3 Results

3.1 Temporal variability of AOD

3.1.1 Interannual variability

Annual average AOD derived from MODIS from 2000 to 2012 is shown in Fig. 2. AODs are all above 0.55 during this period. There are three increasing phases: 2000–2002, 2005–2008, and 2010–2011. The fastest increase occurred from 2005–2008 and the peak AOD value reached 0.68 in 2008. The AOD value started to decline sharply from 2008 to 2010 and reached a minimum value of 0.59 in 2010. The World Expo 2010 was held in Shanghai, at which time the local government expended numerous efforts to protect the environment by controlling air pollutants. The long-term trend of AODs derived from the ensemble empirical mode decomposition (EEMD) analysis, as shown by dashed lines (Fig. 2) , further demonstrated that AOD increased before 2008, followed by a decrease in the CRD (Zhao et al., 2013).

3.1.2 Seasonal variability

AODs are highest in spring (0.71±0.06) and summer (0.74±0.09), as compared to observations in autumn (0.53 ± 0.06) and winter (0.49±0.04) (Fig. 3). This trend suggests that aerosol loadings are higher in spring and summer than in autumn and winter. Additionally, the standard deviation in spring is less than in summer, indicating that the variations of aerosol in spring are smaller than those in summer during the study periods. α in spring (0.86±0.10) is lower than (1.32±0.05) in summer, which indicates the inconsistent patterns of the AODs and α (Fig. 3). AOD value is higher and α value is lower in spring compared to the values in summer, indicating a tendency for the aerosol particles to be coarser. In contrast, aerosol particles tend to be finer in the summer. Figure 4 shows time series of seasonal average AOD and α from 2000 to 2012. AODs in spring and summer are greater than in autumn and winter (Fig. 4(a)). AOD comparisons before 2002 show higher values in spring than in summer. Subsequently, with the exception of 2006 and 2007, AOD values in summer were greater than those in spring thus indicating that large AODs frequently begin to appear in summer. The long-term season variations of α, as shown in Fig. 4(b), describe α values in summer and autumn as greater than those in spring and winter. α values in summer are generally the highest, followed by autumn, indicating obvious seasonal characteristics in the variation of α. In winter and spring, α values are quite similar, but the change range of α in spring is greater than in winter.

3.1.3 Monthly variability

Figure 5 shows the monthly averages of AOD and α from 2000 to 2012. The peak value of AOD of 1.0±0.12 occurred in June, with an opposite result of 0.4±0.05 detected in December. α is high in August (1.46±0.06), which demonstrates the dominance of fine particles in AOD. α is low in April (0.82±0.12), mainly due to the transport of coarse particles from sand-storms in northern China at large-scales. AOD value is highest in June, with α at approximately 1.4, indicating the complexity of aerosol particles components and that they are affected by numerous other factors. AOD value declines sharply after June, opposite to what is observed in α. This is due to the rainy season in CRD during that time, with abundant rainfall resulting in a significant decrease in the lifecycle of aerosol particles, especially those of large-scale.

3.2 Spatial variability of AOD

The spatial distribution of multi-year average AOD during 2000–2012 is shown in Fig. 6. High AODs are mainly distributed in the northern regions of CRD, where the values range from 0.6 to 0.7 in northern Jiangsu and Anhui provinces. This is also the case for the southern regions of Jiangsu Province and Shanghai (0.7–0.8), with high population density and industry development. High AODs are also characteristic in Anhui where dense population and many copper smelting industries are located along the Changjiang River and surrounded by Dabie and Tianmu Mountain. This result is consistent with the results by He et al. (2012), who found that aerosols emitted in this region were difficult to dissipate from 2000 to 2007. Low AODs are mainly located in the southern regions of CRD with values below 0.6. In addition, the altitude has a significant effect on the distribution of AOD. High AODs are distributed in the low-lying plains, as well as the plains along the Changjiang River and Hangzhou Bay. Opposite results are generally observed in mountai-

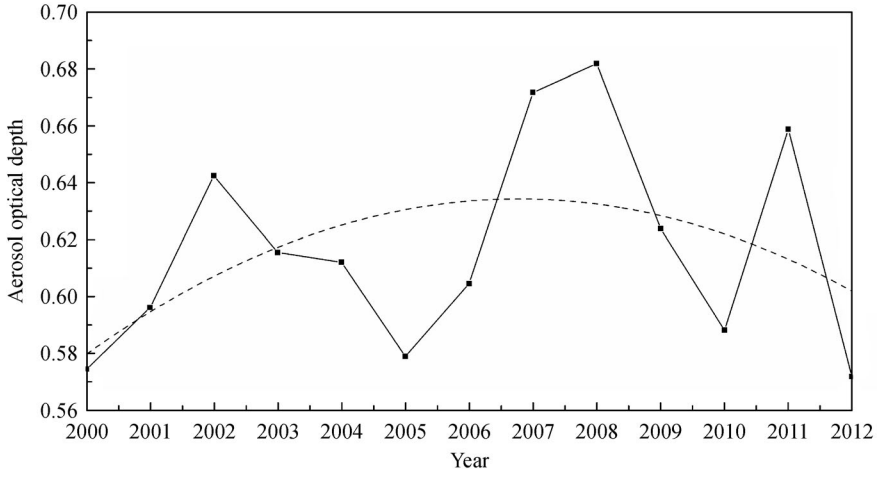

Fig. 2 Annual average AOD derived from MODIS at 550 nm from 2000 to 2012. The dashed line represents the long-term variability trend of the AODs derived from the ensemble empirical mode decomposition (EEMD) analysis.

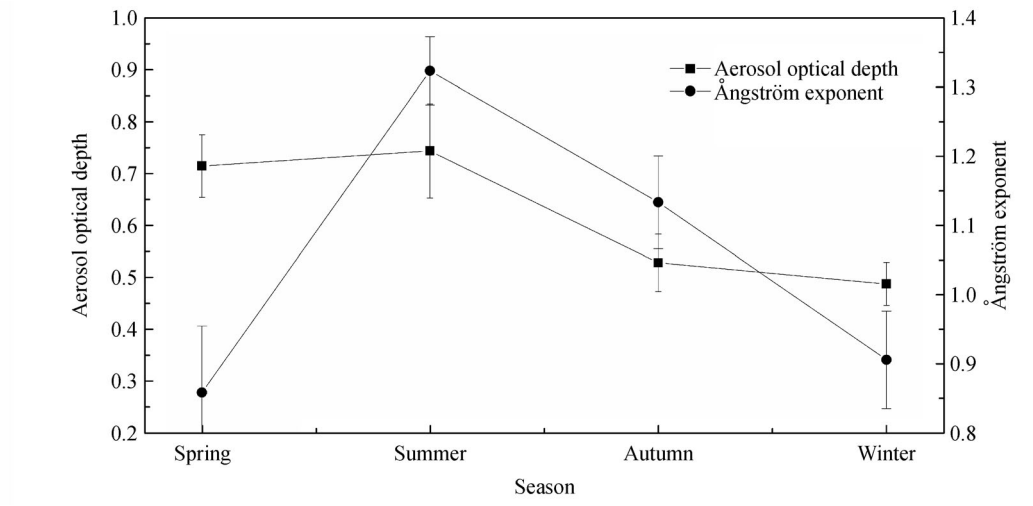

Fig. 3 Multi-year seasonal average AOD at 550 nm and Ångström exponent from 2000 to 2012. The error bars on the dots along *y*-axis denote the standard deviation.

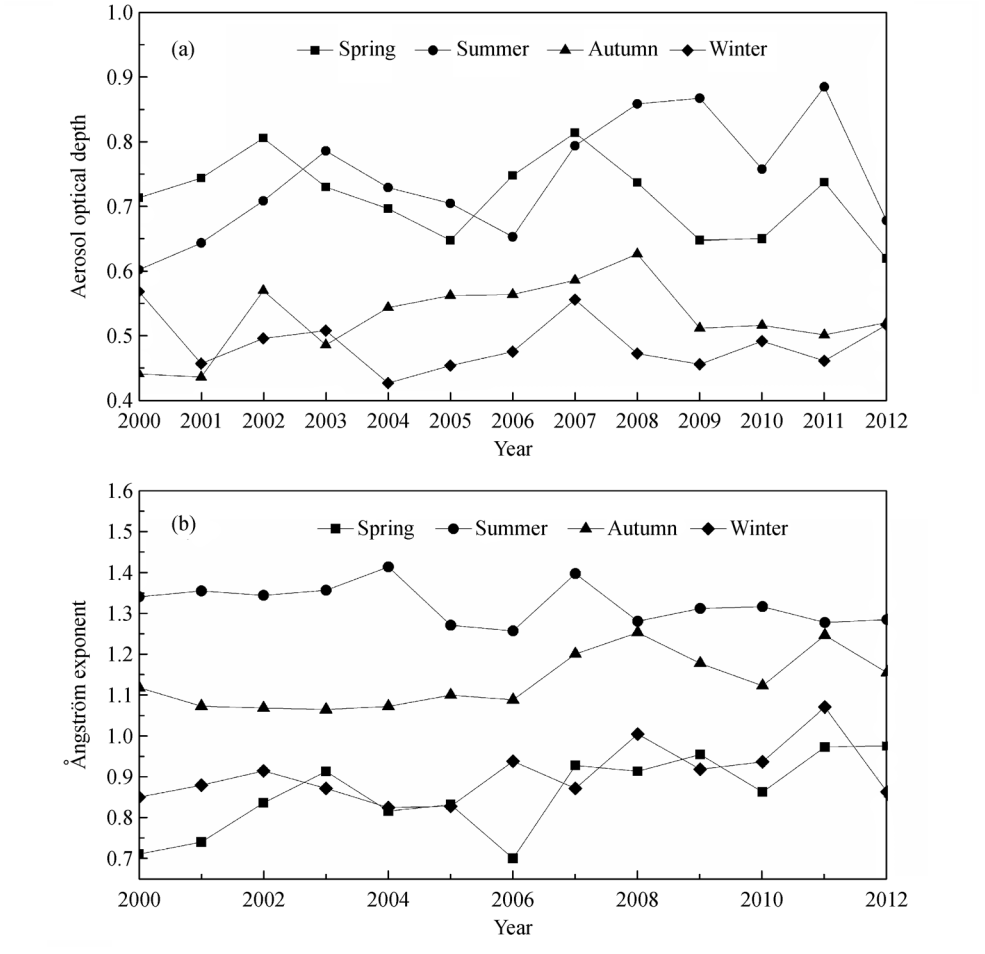

Fig. 4 Seasonal average AOD at 550 nm (a) and Ångström exponent (b) from 2000 to 2012.

nous areas, which are mainly located in southern regions of CRD. The maximum AODs are distributed in Shanghai

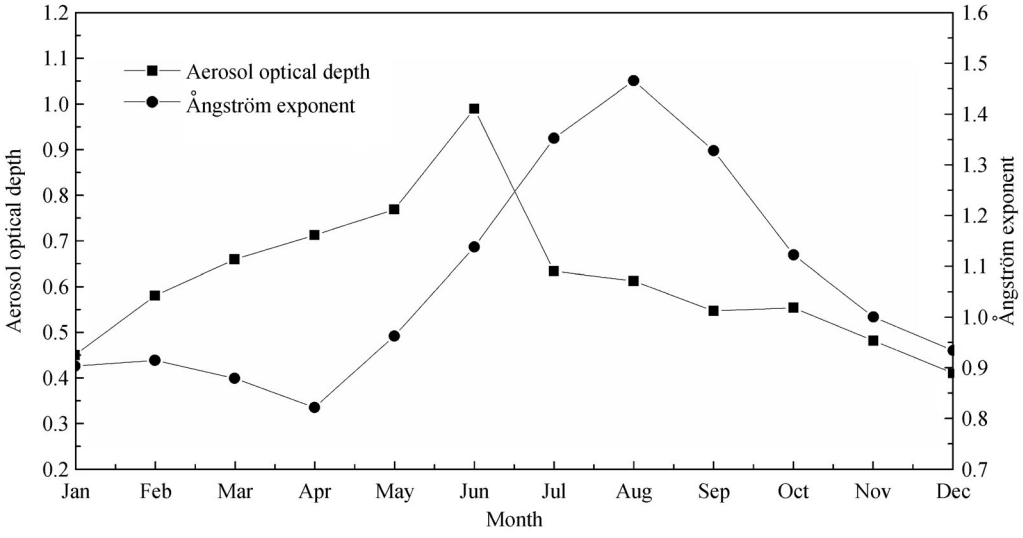

Fig. 5 Monthly average AOD at 550 nm and Ångström exponent from 2000 to 2012.

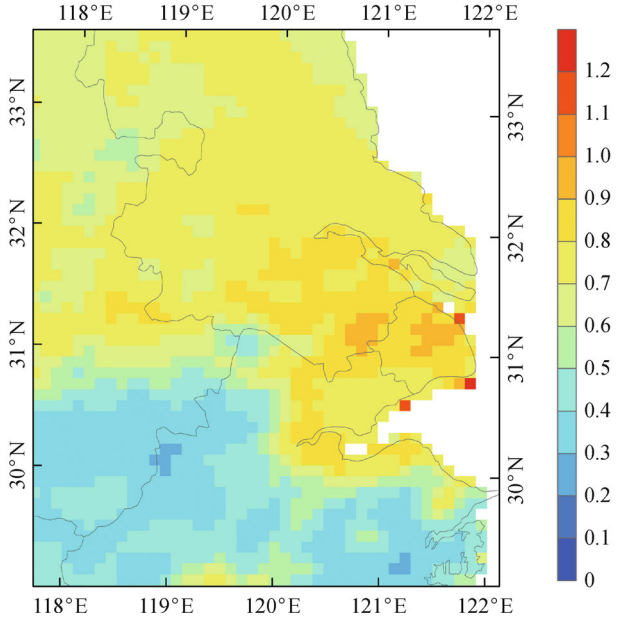

Fig. 6 The spatial distribution of AOD at 550 nm averaged from MODIS from 2000 to 2012 in the Changjiang River Delta.

and its surrounding areas, indicating that a high concentration of human activities are a great contributor to the increase in AODs in these regions.

3.2.1 Interannual spatial variability of AOD

Figure 7 shows the spatial distribution of annual average AOD from 2000 to 2012. The distribution pattern of the AOD in each year is similar to that of distribution patterns over the whole period (Fig. 6). AODs are higher in the northern region of the CRD than in the southern region throughout all periods. High aerosol loadings are mainly distributed in Jiangsu Province, Shanghai, and northern regions of Anhui Province and Zhejiang Province. High population density and highly developed industry are characteristic in these areas, resulting in numerous aerosol emission sources. Low AODs are typically occur in the central region of Zhejiang Province and southern region of Anhui Province.

The aerosol loadings showed an increase from 2000 to 2008 over the CRD, except in 2003, 2004, and 2005. AODs slightly declined in 2003 from 2002. In 2000 and 2001, the high values of AODs generally appeared in the region along Changjiang River. After 2001, Shanghai and its surrounding areas became the central areas with high AODs for all years. There was a sharp increase in AOD during 2006–2007, especially in the northern region of CRD, as opposed to what was detected in 2009 and 2010.

3.2.2 Seasonal spatial variability of AOD and α

Figure 8 shows the spatial distributions of seasonal average AOD and α in the CRD from 2000 to 2012. The maximum AODs generally appeared over the southern region of Jiangsu Province and throughout the Shanghai region during all the seasons. In spring, high AODs were mainly observed in the northern region of CRD. AODs are typically greater than 0.7. The maximum AODs in spring are distributed in the areas along the Changjiang River, Shanghai, and Hangzhou Bay, with a maximum value at approximately 1.0. In summer, aerosols are greater than in spring over the northern region of CRD. AODs are above 0.8 in most regions of northern Anhui, with values typically $\leqslant$1.0 over the Jiangsu Province. The maximum values of AODs appear in Shanghai and its surrounding areas, with the maximum at approximately 1.1. Low AODs

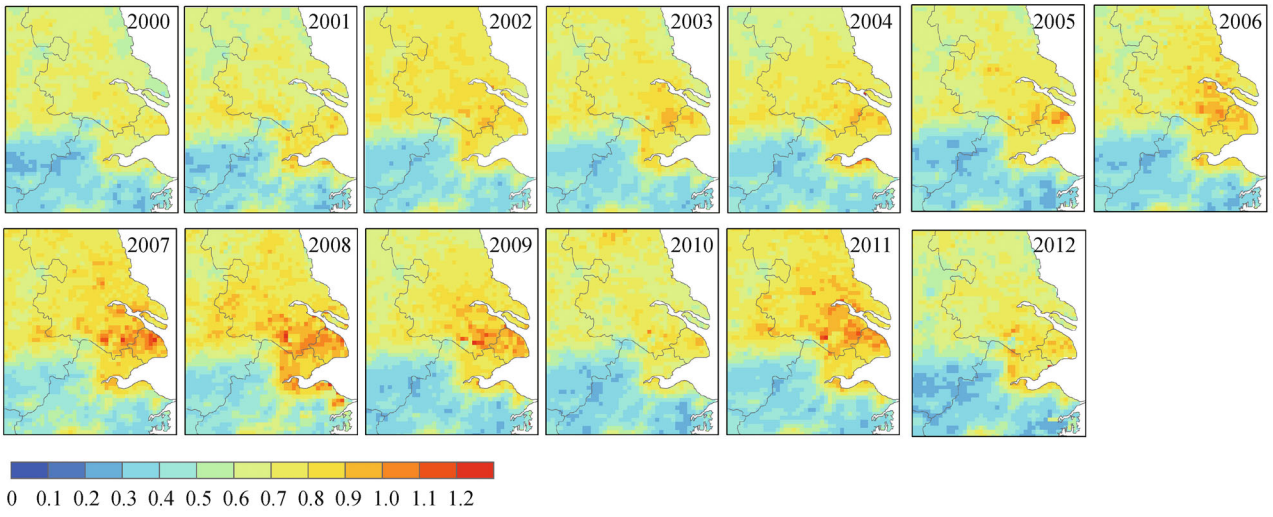

Fig. 7 The spatial distribution of annual average AOD at 550 nm in the Changjiang River Delta from 2000 to 2012.

in the southern region of CRD are relatively stable in both spring and summer, with values between 0.2 and 0.5. However, AODs show a slight decline in summer compared with to spring in the southern region of CRD. The spatial distributions of AOD in autumn and winter are very similar. AODs significantly decline during these two seasons across this region, with values typically below 0.7. AODs are lower in winter than during other seasons over most regions of the CRD.

The α values depend on the size of the aerosol particles, which increases with decreasing particle size (He et al., 2012). Low α values are typically located in the northern plains, and high values are mainly distributed in the mountainous areas (i.e., Anhui and Zhejiang Province). α values are relatively lower in the northern region of CRD than in the southern region, especially in spring and winter. In spring, α values range between 0.6 and 0.1 throughout the CRD, indicating that the aerosol particles are typically coarse. In summer, the α value begins to increase over the whole region. Their values range between 1.0 and 1.4, with some rising above 1.5, over some sections of the northern and southern CRD, respectively, suggesting that fine particles are the main components of AOD. The α values in autumn begin to decrease in the northern region of CRD with values typically below 0.8. However, α values stay relative stable in the southern region of CRD. In winter, the distribution of α is very similar to that in spring, and the aerosol particles are typically coarse.

3.3 Seasonal AOD analyzed by EOFs method

To further analyze the spatio-temporal characteristics of AOD in the CRD, the EOFs method is applied to analyze seasonal averages for a long time series from 2000 to 2012. There are a total of 52 seasonal AOD data images. Although AOD is averaged in each season and each year, some pixel values are still missing due to cloud cover. These missing data are excluded due to their limitations. Effective AOD data are processed into the covariance matrix. The EOFs method is then applied to obtain the dominant modes and the time coefficient to the corresponding EOF modes. Given the time period for the collected data is only thirteen years, the discussion of results mainly focuses on the seasonal variability.

Table 1 shows the explanation of the percentage variance of the five EOF modes. According to North's rule (North et al., 1982), significant error tests for eigenvalues are defined as:

$$\lambda_i - \lambda_{i+1} \geqslant \lambda_i \sqrt{\frac{2}{n}}, \tag{2}$$

where n represents the length of the time series and i represents the eigenvalue. We know the first five eigenvalues can satisfy the inequality. In general, it will choose the first three eigenvalues, because the accumulating contribution rate of the first three eigenvalues reaches 77%. Compared with the accumulating contribution rate of the first four or five eigenvalues, the difference is very small. Therefore, by interpolation, we can obtain the first three modes that correspond to the eigenvalues, as shown in Fig. 9.

The first mode accounts for 67% of the total variance (Table 1), which is much higher than the contribution rates of the other three modes. It can reflect the main characteristic of seasonal AOD in the CRD (Fig. 9(a)). The values are all positive indicating that the performance of the first mode works well. High values in the first mode are mainly located in the northern region of CRD (i.e., northern regions of Anhui, Jiangsu Province, and Shanghai). Alternatively, values of the first mode generally

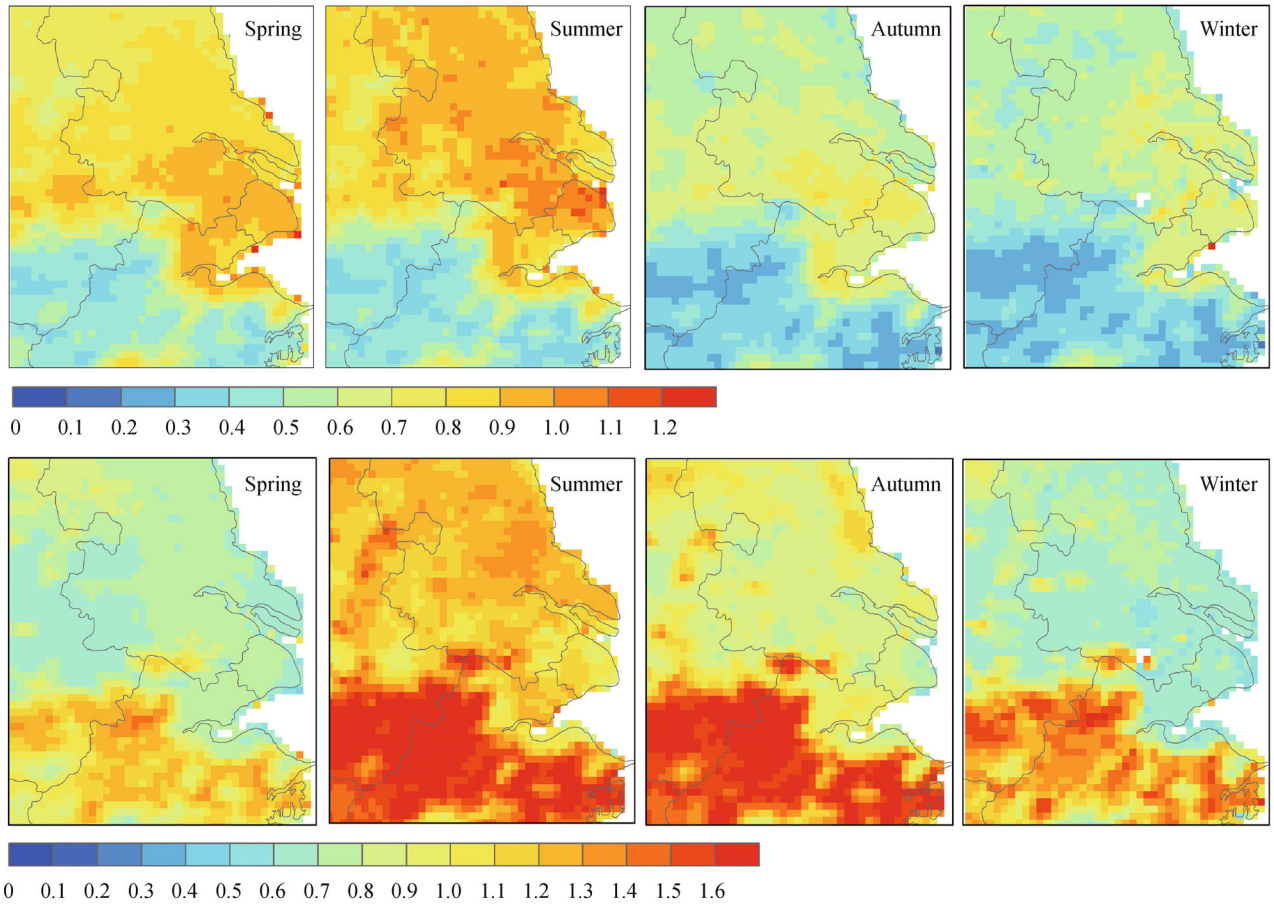

Fig. 8 Spatial distributions of seasonal average AOD at 550 nm (upper panel) and Ångström exponent (lower panel) in the Changjiang River Delta during 2000–2012.

Table 1 Percentage variance explained for the first five empirical orthogonal functions (EOFs) modes.

Principal component	Eigenvalue	Contribution rate/%	Accumulating contribution rate/%
1	24.95	66.88	66.88
2	2.67	7.16	74.04
3	1.11	2.97	77.01
4	0.82	2.19	79.20
5	0.64	1.73	80.93

decrease from the northern to the southern regions, with the lowest values generally observed in the south. The distribution shown in the first mode fits well with the spatial distribution of altitude and population density. The time coefficient that corresponds to the first mode reflects the entire variability trend of seasonal AOD (Fig. 10(a)). High aerosol loadings typically appear in spring and summer, as opposed to what is observed in autumn and winter. The variability of time has an obvious seasonal cycle. Figure 9(b) shows that the second mode accounts for 7% of the total variance. Changjiang River is regarded as the zero dividing line. Its values are positive in the northern region of Changjiang River and negative in the south, indicating opposite AOD results in these two areas. According to the time coefficient corresponding to the second mode (Fig. 10(b)), most of the summer and winter values are positive. Figure 9(c) shows that the third mode accounts for 3% of the total variance. The values of the third mode are positive in the southeast and negative in the northwest. As shown from the time coefficient corresponding to the third mode (Fig. 10(c)), even with a slight change in values and the periodic variation not obvious, almost all spring and winter values are positive. In other seasons, most values are negative.

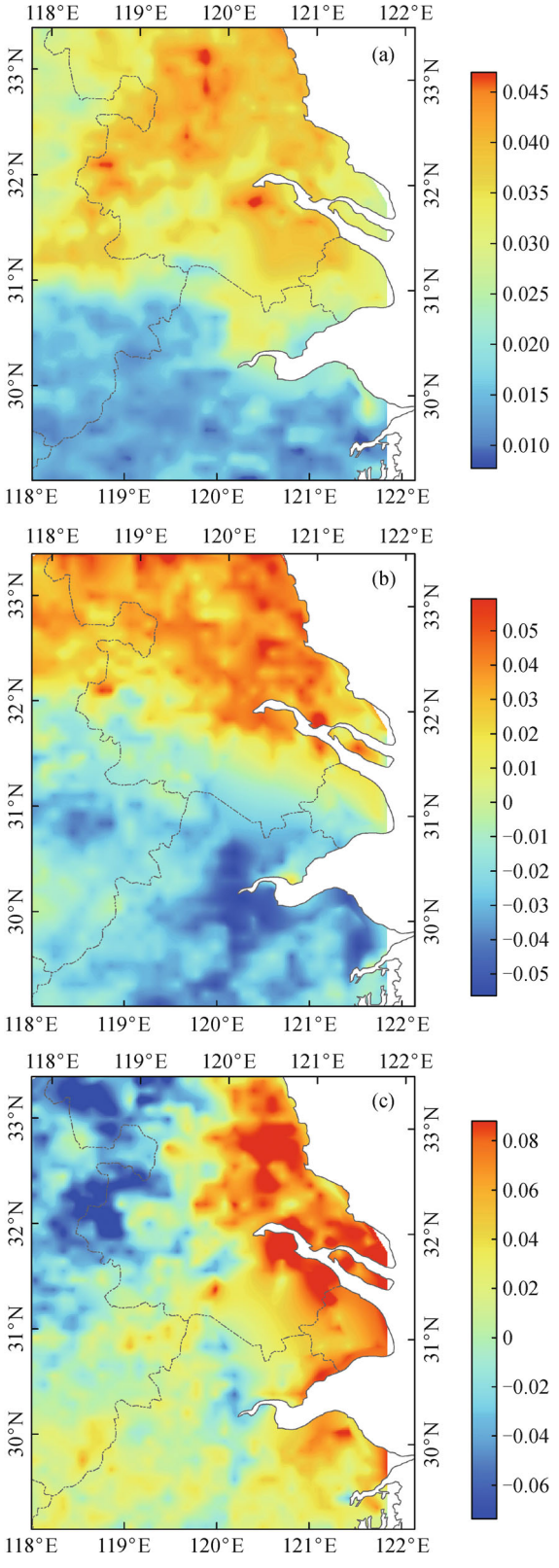

Fig. 9 Spatial modes of seasonal AOD in the Changjiang River Delta by the empirical orthogonal functions (EOFs), i.e., (a) the first EOF mode, (b) second EOF mode, and (c) third EOF mode.

4 Discussion

The main objective of this study is to analyze the temporal and spatial variability of AOD over the CRD from 2000 to 2012. The variability of annual average AOD showed an increasing trend from 2000 to 2008, followed by a decrease (Fig. 2), suggesting that aerosol loadings have improved in recent years. AODs were higher in 2006 than in 2005, likely due to the occurrence of frequent sand-storms from northern China. According to the sand-dust weather statistics drawn by Duan et al. (2013), 18 and 17 sand-dust weather processes occurred in the spring seasons (MAM) of 2006 and 2007, respectively, relative to the long-term mean values. Combined with the spatial variability of annual AOD (Fig. 7), the most obvious change is detected in Shanghai. In 2010, aerosol loadings were low compared to the values of previous years. This is consistent with results reported by Zhao et al. (2013), who found AOD significantly decreased during the World Expo 2010 in Shanghai from 2000 to 2011, indicating a remarkable improvement in air quality in Shanghai during World Expo 2010.

From the temporal and spatial variability of seasonal AOD, one can conclude that AOD has obvious seasonal variability in the CRD. Studies have shown that rapid economic development, industrial pollution, and automobile exhaust emissions led to an increase of aerosol in these areas (Deng et al., 2010). High AODs were observed in spring and summer, as opposed to the low AODs observed in autumn and winter (Fig. 7). Given it has been shown that climate in the CRD is typically affected by East Asian monsoons, it can be assumed that other meteorological factors may also influence the temporal and spatial variability of aerosols in different seasons. According to the variability of α, aerosol particles are consistently coarse in spring and winter and are dominated by fine particles in summer and autumn. In spring, aerosol loadings are high, likely due to the frequent occurrence of sand-storms. In addition, prevailing western winds are conducive to the transportation of aerosols from the inland. Increased human activities during the summer result in high aerosols. Relative humidity and high temperatures can promote gas-to-particle conversion to aerosols. An additional cause for increased aerosols in summer is from anthropogenic aerosol emissions. The CRD is one of the most important agricultural regions in China. The summer harvest and the burning of straw and subsequent residues have the potential to emit large amounts of particles, which can lead to a serious increase in air pollution (Su et al., 2012). In addition, abundant precipitation brought on by summer monsoons can reduce the amount of coarse particles in the air. AODs rapidly decrease in autumn and winter due to aerosol loadings which are strongly influenced by fast-moving synoptic weather patterns (Kim et al., 2007). The

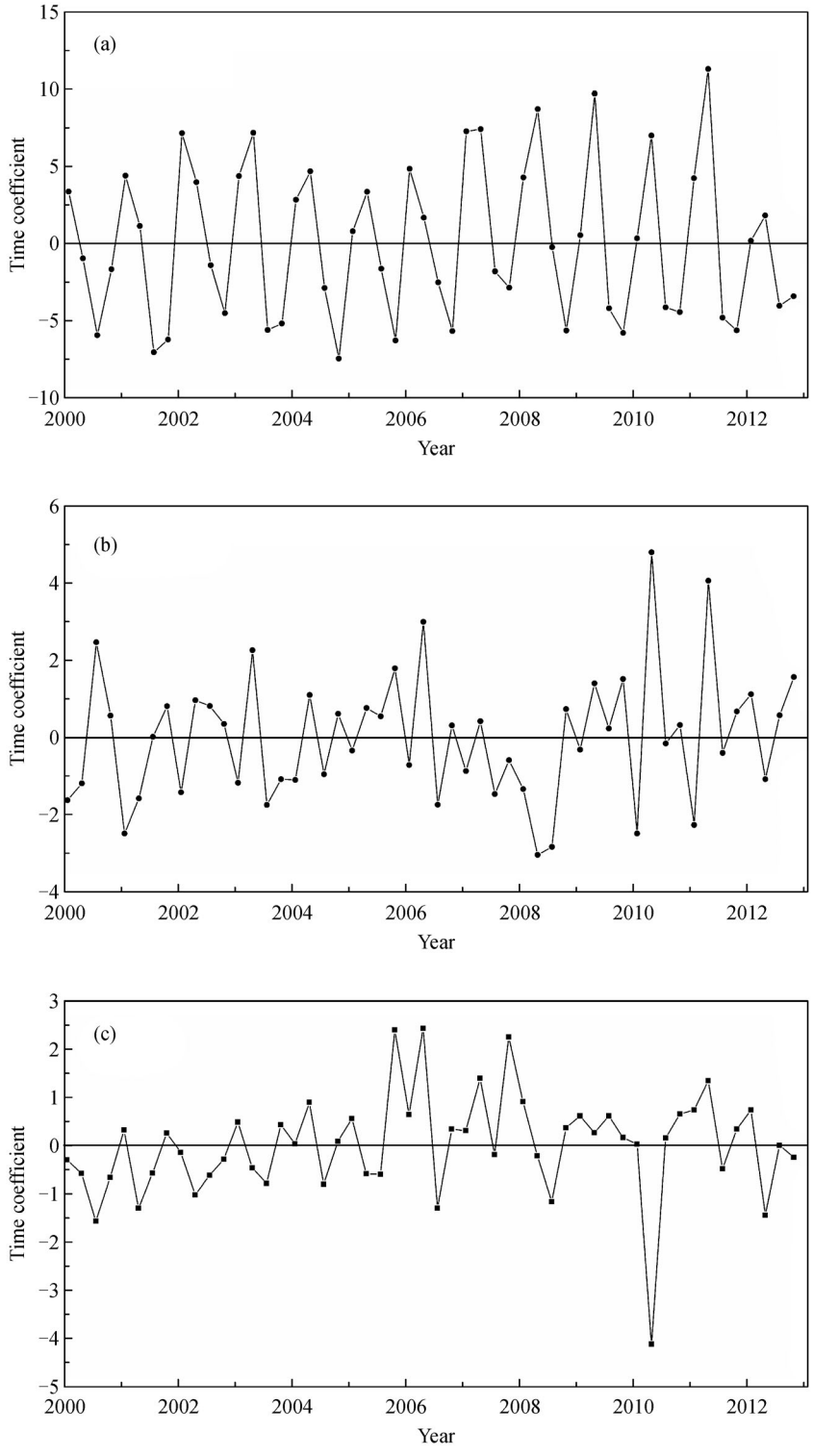

Fig. 10 Time coefficients corresponding to the EOF modes: (a) first mode; (b) second mode; and (c) third mode.

prevailing northwestern wind is conducive to the spread of aerosols, possibly at large-scales.

In this paper, we have further discussed the seasonal distribution characteristics of aerosols by the EOFs method. The three modes account for 67%, 7%, and 3% of the total variance respectively, along with their corresponding time coefficients. The first mode explains the distribution pattern of aerosols in the CRD in all seasons, showing similar distributions in spring and summer, with stronger contributions to aerosols. The

second mode primarily explains summer and winter distribution patterns. The CRD is located in the subtropical monsoon climate zone where wind direction and speed can significantly affect regional aerosol distributions. The CRD is near the East China Sea where the prevailing wind direction in summer is from the south-southeast which can bring ocean air inland and decrease AOD loadings. By comparison, the prevailing northwestern wind in winter can easily spread aerosols from inland areas to the southeast sections of the CRD, resulting in an increase in AODs. In the third mode, the values along the coast are positive and are negative in inland areas. This distribution of aerosols usually occurs in spring and winter when the prevailing west-northwest winds could bring aerosol particles from inland area to the main body of CRD.

5 Conclusions

In this study, we analyze the spatial distribution and temporal variability of AOD and Ångström exponent in the CRD, using the data taken from US Terra satellite MODIS from 2000 to 2012 and the EOFs analysis. The results are summarized as follows.

1) Spatially, high AODs are mainly distributed in the low-lying plains and basins, with opposing results detected in the mountainous areas. High AODs are also observed along the coastal areas and the Changjiang River.

2) Temporally, AODs have generally increased over the last decade. This is especially true for the northern regions of the CRD. AOD also shows seasonal variability, i.e., high AODs are detected in spring and summer, as opposed to the low AODs observed in autumn and winter.

3) Coarse particles are the AOD dominant components in spring, which are likely affected by the transport of sand dust from north China. In contrast, fine particles are the dominant AOD components in summer, likely due to the anthropogenic aerosols.

4) AODs decreased during the World Expo 2010 in Shanghai and its surrounding areas. It is reasonable to attribute this decrease to the strong air pollution control measures imposed by the local government.

5) The spatial and temporal patterns of seasonal AODs show that the first three EOF modes cumulatively account for 77% of the total variance. The first mode that explains 67% of the total variance shows the primary spatial distribution of aerosols, i.e., high AODs are distributed in the northern areas and low AODs in the southern areas. The second mode (7%) shows that the monsoon climate likely plays an important role in modifying the distribution of aerosols, especially in summer and winter. The third mode (3%) shows aerosol distribution in spring and winter when the prevailing west-northwest wind could possibly spread aerosol particles from the inland areas into the main body of CRD.

Acknowledgements The authors gratefully acknowledge NASA Langley Research Center Atmosphere Sciences Data Center for distributing MODIS data. The research was partially supported by Shanghai Science and Technology Support Program—Special for EXPO (Grant No. 10DZ0581600), Research Grants of Science and Technology Commission of Shanghai Municipality through Project 13ZR1453900 and 13231203804, the Fundamental Research Funds for the Central Universities, a grant from Shanghai Institute of Urban Ecology and Sustainability, and Research Grant of Key Laboratory of Geographical Information Science, Ministry of Educution, East China Normal University through Project KLGIS 2013C02.

References

Ångström A (1929). On the atmospheric transmission of sun radiation and on dust in the air. Geogr Anal, 12: 130–159

Chu D A, Kaufman Y J, Ichoku C, Remer L A, Tanr D, Holben B N (2002). Validation of MODIS aerosol optical depth retrieval over land. Geophys Res Lett, 29(12): 8007

Deng X, Deng W, He D (2010). Spatial-temporal features of atmospheric aerosol in East China in recent years. Transactions of Atmospheric Sciences, 33(3): 347–354 (in Chinese)

Duan H, Zhao J, Li Y (2013). The frequencies, severities, and driving factors of the sand-dust weather processes occurred in Northern China in the spring of 2011. J Desert Res, 33(1): 179–186 (in Chinese)

Duan X, Yu X, Liu X (2009). Analysis on the character of regional development of 30 years in the Yangtze River Delta. Econ Geogr, 29 (2): 185–192 (in Chinese)

Eck T F, Holben B N, Reid J S, Dubovik O, Smirnov A, O'Neill N T, Slutsker I, Kinne S (1999). Wavelength dependence of the optical depth of biomass burning, urban, and desert dust aerosols. J Geophys Res, 104(D24): 31333–31349

Engel-Cox J A, Holloman C H, Coutant B W, Hoff R M (2004). Qualitative and quantitative evaluation of MODIS satellite sensor data for regional and urban scale air quality. Atmos Environ, 38(16): 2495–2509

He Q, Li C, Geng F, Lei Y, Li Y (2012). Study on long-term aerosol distribution over the land of East China using MODIS data. Aerosol and Air Quality Research, 12(3): 304–319

He Q, Li C, Tang X, Li H, Geng F, Wu Y (2010). Validation of MODIS derived aerosol optical depth over the Yangtze River Delta in China. Remote Sens Environ, 114(8): 1649–1661

Holben B N, Eck T F, Slutsker I, Tanré D, Buis J P, Setzer A, Ver-mote E, Reagan J A, Kaufman Y J, Nakajima T, Lavenu F, Jankowiak I, Smirnov A (1998). AERONET—A federated instrument network and data archive for aerosol characterization. Remote Sens Environ, 66(1): 1–16

Holben B N, Tanré D, Smirnov A, Eck T F, Slutsker I, Abuhassan N, Newcomb W W, Schafer J S, Chatenet B, Lavenu F, Kaufman Y J, Castle J V, Setzer A, Markham B, Clark D, Frouin R, Halthore R, Karneli A, O'Neill N T, Pietras C, Pinker R T, Voss K, Zibordi G (2001). An emerging ground-based aerosol climatology: aerosol optical depth from AERONET. J Geophys Res, 106(D11): 12067–12097

Hu T, Sun Z, Zhang H (2008). Spatial/Temporal variations and trends of aerosol optical depth at 380 nm wavelength in China during 1980–

2001. Journal of Applied Meteorological Science, 19(5): 513–521 (in Chinese)

Ichoku C, Chu D A, Mattoo S, Kaufman Y J, Remer L A, Tanré D, Slutsker I, Holben B N (2002). A spatio-temporal approach for global validation and analysis of MODIS aerosol products. Geophys Res Lett, 29(12): 8006

Kaskaoutis D G, Kambezidis H D, Adamopoulos A D, Kassomenos P A (2006). On the Characterization of aerosols using the Ångström exponent in the Athens area. J Atmos Sol Terr Phys, 68(18): 2147–2163

Kaufman Y J, Tanré D, Boucher O (2002). A satellite view of aerosols in the climate system. Nature, 419(6903): 215–223

Kaufman Y J, Tanré D, Remer L A, Vermote E F, Chu A, Holben B N (1997). Operational remote sensing of tropospheric aerosol over land from EOS moderate resolution imaging spectroradiometer. J Geophys Res, D, Atmospheres, 102(D14): 17051–17067

Kennedy I M (2007). The health effects of combustion-generated aerosols. Proc Combust Inst, 31(2): 2757–2770

Kim H S, Chung Y S, Lee S G (2013). Analysis of spatial and seasonal distributions of MODIS aerosol optical properties and ground-based measurements of mass concentrations in the Yellow Sea region in 2009. Environ Monit Assess, 185(1): 369–382

Kim S W, Yoon S C, Kim J, Kim S Y (2007). Seasonal and monthly variations of columnar aerosol optical properties over East Asia determined from multi-year MODIS, LIDAR, and AERONET Sun/sky radiometer measurements. Atmos Environ, 41(8): 1634–1651

King M D, Kaufman Y J, Menzel W P, Tanré D (1992). Remote sensing of cloud, aerosol, and water vapor properties from the moderate resolution imaging spectrometer (MODIS). IEEE Trans Geosci Rem Sens, 30(1): 2–27

King M D, Kaufman Y J, Tanré D, Nakajima T (1999). Remote sensing of tropospheric aerosols from space: past, present, and future. Bull Am Meteorol Soc, 80(11): 2229–2259

King M D, Menzel W P, Kaufman Y J, Tanré D, Gao B, Platnick S, Ackerman S A, Remer L A, Pincus R, Hubanks P A (2003). Cloud and aerosol properties, precipitable water, and profiles of temperature and water vapor from MODIS. IEEE Trans Geosci Rem Sens, 41(2): 442–458

Levy R C, Remer L A, Tanré D, Mattoo S, Kaufman Y J (2009). Algorithm for Remote Sensing of Tropospheric Aerosol over Dark Targets from MODIS: Collections 005 and 051: Revision 2; Feb 2009

Li C, Lau A K H, Mao J, Chu D A (2005). Retrieval, validation, and application of the 1km aerosol optical depth from MODIS measurements over Hong Kong. IEEE Trans Geosci Rem Sens, 43 (11): 2650–2658

Li C, Mao J, Lau K H A, Chen J, Yuan Z, Liu X, Zhu A, Liu G (2003). Characteristics of distribution and seasonal variation of aerosol optical depth in eastern China with MODIS products. Chin Sci Bull, 48(22): 2488–2495

North G R, Bell T L, Cahalan R F, Moeng F J (1982). Sampling errors in the estimation of empirical orthogonal functions. Mon Weather Rev, 110(7): 699–706

Pan L, Che H, Geng F, Xia X, Wang Y, Zhu C, Chen M, Gao W, Guo J (2010). Aerosol optical properties based on ground measurements over the Chinese Yangtze Delta Region. Atmos Environ, 44(21–22): 2587–2596

Pope C A 3rd, Dockery D W (2006). Health effects of fine particulate air pollution: lines that connect. J Air Waste Manag Assoc, 56(6): 709–742

Preisendorfer R W, Mobley C D (1988). Principal component analysis in meteorology and oceanography. Amsterdam: Elsevier

Qiu J, Yang L (2000). Variation characteristics of atmospheric aerosol optical depths and visibility in North China during 1980–1994. Atmos Environ, 34(4): 603–609

Remer L A, Kaufman Y J, Tanré D, Mattoo S, Chu D A, Martins J V, Li R R, Ichoku C, Levy R C, Kleidman R G, Eck T F, Vermote E, Holben B N (2005). The MODIS aerosol algorithm, products, and validation. J Atmos Sci, 62(4): 947–973

Shrestha P, Barros A P (2010). Joint spatial variability of aerosol, clouds and rainfall in the Himalayas from satellite data. Atmos Chem Phys, 10(17): 8305–8317

Su J, Zhu B, Kang H, Wang H, Wang T (2012). Applications of pollutions released from crop residues at open burning in Yangtze River Delta Region in air quality model. Environ Sci, 33(5): 1418–1424 (in Chinese)

Yang K L (2002). Spatial and seasonal variation of PM10 mass concentrations in Taiwan. Atmos Environ, 36(21): 3403–3411

Zhao Q, Gao W, Xiang W, Shi R, Liu C, Zhai T, Huang H A, Gumley L E, Strabala K (2013). Analysis of air quality variability in Shanghai using AOD and API data in the recent decade. Front Earth Sci, 7(2): 159–168